DYNAMICS OF POTENTIAL FUNCTIONALITY OF OBJECTS

Tadeusz KRUPA
Warsaw University of Technology, Faculty of Management, Warsaw, POLAND
e-mail: tadeusz.krupa@pw.edu.pl

Abstract: This article guides the reader through the seemingly simple issues of the assessment, protection and transfer of the potentials of an object's functionality through its internal and external buffers, by employing Cartesian multiplication and signatures. The change in the potentials of buffers and the functionality of objects is the focus of this research, guaranteeing the correct use of potentials in relation to the whole "shell" of the object. In order to avoid any collision in the transport of functional potentials, each proper buffer is, by definition, connected to one and only one object. On the probability scale Σ [0..1], the potential of the object's functionality is expressed as the system sum [0..1] of all the potentials of its proper buffer components. A practical and important part of the article contains two methodologically important examples of tabular construction and analysis: an example of the dynamics of the potentials of an object with two buffers, together with a table of the potentials of a two-buffer object; and an example of the Cartesian product of graphs with lost determinism together with the table of potentials of a two-buffer object with an extensive option structure.

Keywords: proper buffer, dynamics of object potentials; ergodic potential of functionality, Cartesian product, system sum, complexity of calculations.

JEL: C4, C5.

1 Introduction

The design of a system can be understood as a set of objects connected to each other by means of buffers that remain inside the objects and, externally, connected between the objects for the processes of maintaining memory buffers that operate in such a way that they can also communicate in a unified way, both transmitting between the buffers and protecting the functional potentials.

These high-level connections require the definition and acceptance of a complementary group of constraints, such that compliance with the constraints ensures the balance, openness and uniformity of cooperation of the objects. This is achieved, first, with the help of Cartesian graph multiplication tools and their signatures, and, second, by using the high-complexity characterization theories[1].

System objects can have both internal and external buffers of functional potentials. The functional potentials of an object are determined on the basis of the probability of potential changes in the buffers of the whole object, as well as on the basis of the probability of the current functional potentials of each buffer, in order to maintain the balance of the probabilities of the current functionality of the entire facility. This setup is illustrated by means of Cartesian calculus, using the products of the graphs describing the sequences of probabilities of the states of the whole object.

The functionality of the external buffers of the object can be extended to other objects, which, in practice, means that the current probabilities of the potentials of a given functionality are shared with other objects, cached by buffers. The potentials of useful functionality can be collected and used by objects in a percentage range of 1% to 100%.

For the processing of the functional potentials within the limits of the available potential of the object, only the internal buffer potentials of the object can be considered. The potentials of the external buffers are assumed, a priori, to be involved in the coordina-

[1] The paradigm of Gorbatov's characterization theory is a set of functional-structural relationships for which there are so-called prohibited graph figures, whose liquidation by splitting the minimum number of nodes leads to a structure free of ambiguity errors.

tion of external objects and treated as unavailable directly for internal purposes.

2 Dynamics of buffer potentials and n-buffer objects

For our analyses, the changes of discrete functional potentials from B_j buffer repositories and n-channel O_i objects are focused upon. In order to avoid any misunderstandings, each buffer is connected to one and only one object, externally or internally, by means of an abstract channel represented uniquely by the buffer and its identifier. The mathematical apparatus of the Cartesian product of graphs and the concept of the signature of a graph in Cartesian product operations are employed for the analyses.

For the graphic illustration of the dynamics of the potentials of O_i objects and the B_j buffers connected to them, circles are used, with the necessary symbolism of their position in relation to objects. The potential of the functionality assigned to a buffer is expressed on the probability scale [0..1]. Similarly, on the probability scale [0..1], the potential of the functionality of the object is expressed as the sum of all the potentials of its proper buffers in the system. The procedure for calculating the system total will be illustrated later in the article.

It is assumed that an object has a limited number of internal potentials, determined by the probability of its use and depending only on the ergodic invariance of the level of buffer potentials of this object. An ergodic process is a stationary process for which the values of the statistical parameters for the set of realizations (i.e. the average value, variance and autocorrelation function) are equal to the values of these parameters from its arbitrary implementation.

N-buffer objects (in the special two-buffer case) can be combined into chains or loops, as illustrated in Figs. 1 and 2.

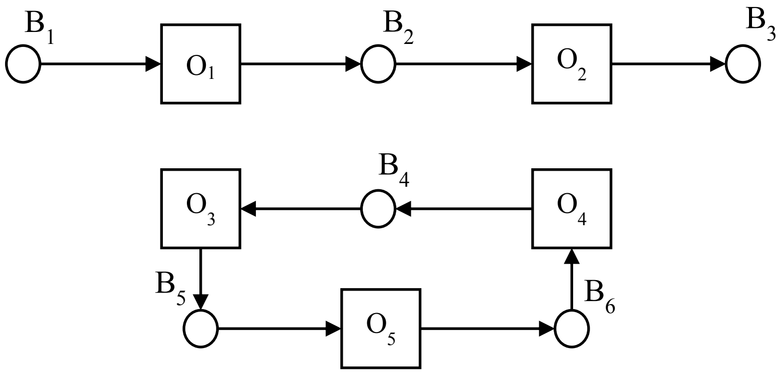

Figure 1. Chain of two objects and a loop of three two-buffer objects, where the buffers B_2, B_3, B_4, B_5 and B_6 are the proper buffers for the objects O_1, O_2, O_4, O_3 and O_5
(*Source:* Authors own research)

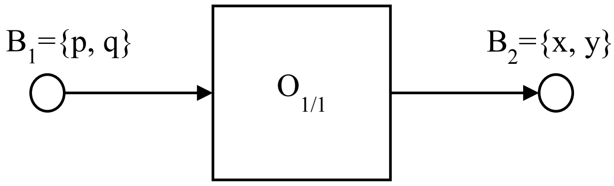

Figure 2. An $O_{1/1}$ object with one input buffer B_1 and one output buffer B_2
(*Source:* Authors own research)

The $O_{1/1}$ object presented in Fig. 2 is characterized by one input buffer, with functional potentials p and q, and one proper buffer with functional potentials x, y.

Buffers $B_1 = \{p, q\}$ and $B_2 = \{x, y\}$ are carriers of functional potentials with ergodic probabilities of their maintenance. The capacities of the buffers B_1 and B_2 can multiply the complexity of the functional potential calculations. If we increase the buffer capacity of the object under consideration by only a factor of 4, it will generate approximately 40,000 combinations of 8-character potential identifiers for each of the two-object buffers, which can lead to an avalanche-like increase in the number of combinations of potential identifiers.

In the present article, the further analysis of the functional potential space will be limited to a small number of proper (initial) buffers and to two or three distinguishable buffer functionalities. These limitations may prove to be an obstacle to the application of the concept of signature on a larger scale in Cartesian product operations on stochastic sets of functional potentials.

The modeling and detailed analysis of the potential changes on the two buffers of the $O_{1/1}$ object presented in Fig. 2 is the starting point for the identification and assessment of the operation of objects with buffers of type B_1–B_2, where the buffer symbol B_1–B_2 represents sets of permissible functional potentials on the proper buffers, causing and simultaneously caused by changes in the value of the probabilities of potentials available in the proper buffers.

The symbols of the potentials of the functionalities p, q, ..., x, y of the buffers (as well as the objects) are assigned, as their actual value, the estimated probability of their current maintenance.

3 Dynamics of object potentials with two buffers

The dynamics of the potentials in two external buffers B_1, B_2 will be illustrated by the graphs G_1, G_2 shown in Fig. 3, where ΓV_1 and ΓV_2 are the signatures of the vertices V_1 and V_2 of the graphs G_1 and G_2, respectively, with potential volatility and signatures presented in the formulas (1, 2).

$$\Gamma V_1 = \{\Gamma p, \Gamma q\} = \{\{p, q\}, \{p\}\}$$
$$\Gamma V_2 = \{\Gamma x, \Gamma y\} = \{\{x, y\}, \{x\}\} \quad (1)$$

which we interpret as follows:

$$\Gamma p = \{p, q\}; \quad \Gamma q = \{p\}$$
$$\Gamma x = \{x, y\}; \quad \Gamma y = \{x\} \quad (2)$$

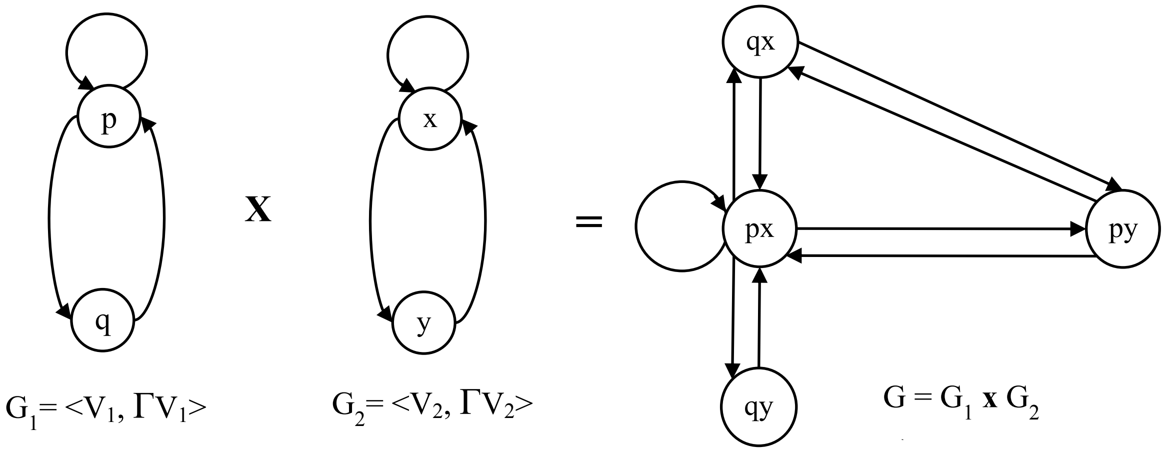

Figure 3. Potential dynamics of a two-buffer object represented by the vertices V_1 and V_2 of the graphs G_1 and G_2, written in the form of a Cartesian product $G_1 \times G_2$, where the symbol × written in bold type indicates the Cartesian product of the two reproduced sets G_1 and G_2 (*Source:* Authors own research)

Fig. 3 presents the graph G with the set of vertices $V = V_1 \times V_2$ and the sets of edges $\Gamma V = \Gamma V_1 \times \Gamma V_2$, which are the Cartesian products of the vertices and the edges of the graphs G_1 and G_2. The graph G and its characteristics are used to study the behavior of the dynamic potentials of the two-buffer object B_1–B_2 that is being considered.

The fully formulated four-potential graph G is shown in Fig. 4. The G graph was constructed as a Cartesian product of the tops of $G_1 \times G_2$ graphs and as a Cartesian product of the edge forms of the potentials of both these graphs.

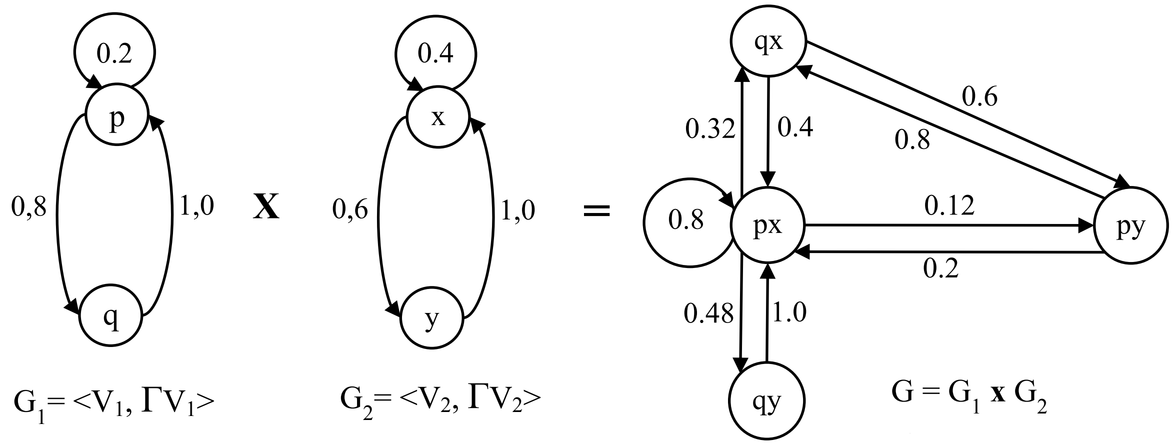

Figure 4. The resulting form of the stochastic graph G of the potentials, written in the form of the Cartesian product of the $G_1 \times G_2$ potential graphs (Source: Authors own research)

Fig. 3 is accompanied by Fig. 4, which shows the probability values of the changes in these potentials (interpreted as potential "a" changes to potential "b" with probability = 0.5) respectively with values:

- for the G_1 graph

$p \to p = 0.2$ $p \to q = 0.8$ $q \to p = 1.0$

$x \to x = 0.4$ $x \to y = 0.6$ $y \to x = 1.0$

- for the G_2 graph

$x \to x = 0.4$ $x \to y = 0.6$ $y \to x = 1.0$

$x \to x = 0.4$ $x \to y = 0.6$ $y \to x = 1.0.$

The vertices of the graph G are formed as the product of the Cartesian vertices of graphs G_1 and G_2 in the following manner:

$$V = V_1 \mathbf{x} V_2 = \{p, q\} \mathbf{x} \{x, y\} = \{px, py, qx, qy\} \quad (3)$$

The edges of the graph G are created using the signature vertices ΓV of the graph G:

$$\Gamma V = \{\Gamma px, \Gamma py, \Gamma qx, \Gamma qy\} \quad (4)$$

where:

$\Gamma px = \Gamma p \mathbf{x} \Gamma x = \{p, q\} \mathbf{x} \{x, y\} = \{px, py, qx, qy\}$

$\Gamma py = \Gamma p \mathbf{x} \Gamma y = \{p, q\} \mathbf{x} \{x\} = \{px, qx,\}$

$\Gamma qx = \Gamma q \mathbf{x} \Gamma x = \{p\} \mathbf{x} \{x, y\} = \{px, py\}$

$\Gamma qy = \Gamma q \mathbf{x} \Gamma y = \{p\} \mathbf{x} \{x\} = \{px\}$

4 Table of potentials of a two-buffer object

The set of observation tables presented below from the ΓV signature are used to build the potential graph of the object, modeled using the Cartesian product of G_1 **x** G_2 graphs with the probability values shown in Fig. 4. The method of constructing a stochastic state graph is universal, illustrated successively with the help of Tables 1 to 4. The number of tables necessary to carry out the entire calculation is equal to the number of potential "graph" summits constructed as a result of multiplying all the graphs of the potentials of objects occurring in the entire modeled object.

The events initiating the potentials px, py, qx, qy - as the available potentials of the $G_1 \times G_2$ object - are obtained using the expression (3). The total value of 1.00 is a control value used to check the correctness of the results of the event observations of the individual potentials, and at the same time is a component of the system sum of all four buffer potentials of the analyzed dynamics of the object modeled by the product $G_1 \times G_2$.

The graph G of the states of the two-buffer object, presented as an object in Fig. 2 and as a graph of states in Fig. 4, is the result of the Cartesian product of stochastic components - vertices and edges of $G_1 \times G_2$ state graphs.

Table 1. Observation of events px

Initializing events	Observation of secondary events	Probability P on the scale [0..1]
px	px → px = 0.2 × 0.4	0.08
	px → py = 0.2 × 0.6	0.12
	px → qx = 0.8 × 0.4	0.32
	px → qy = 0.2 × 0.4	0.48
		Σ=1.00

Table 2. Observation of events py

Initializing events	Observation of secondary events	Probability P on the scale [0..1]
py	py → px = 0.2 × 1.0	0.20
	py → qx = 0.8 × 1.0	0.80
		Σ=1.00

Table 3. Observation of events qx

Initializing events	Observation of secondary events	Probability P on the scale [0..1]
qx	qx → px = 1.0 × 0.4	0.40
	qx → py = 1.0 × 0.6	0.60
		Σ=1.00

Table 4. Observation of events qy

Initializing events	Observation of secondary events	Probability P on the scale [0..1]
qy	qy → px = 1.0 × 1.0	1.00
		Σ=1.00

The proposed procedure can be used to build graphs that describe the dynamics of states of single or multiple objects with distinguished proper buffers, which aid in the analysis of the structure of a functioning object on the basis of Cartesian products of variability of states occurring on its external input and output buffers.

Two examples of Cartesian graphs are presented below:

- with lost capacity of determinism to indicate, unambiguously, decisions on the G_X graph resulting from the Cartesian product of $G_1 \times G_2$ (Example 1),
- with lost semantics – destiny (Example 2).

5 Cartesian products of graph states with lost capacity (determinism): Example 1

The Cartesian products of graph states, or, more precisely, graph operating models, can be used effectively to detect errors, either a priori (resulting from imprecisely defined structural assumptions) or a posteriori (resulting from wrong decisions or even procedural errors), arising in the initial phase of the multiplication of graph models of functioning.

To illustrate the possibilities of Cartesian products, we will use a simple example of the graph synthesis of the states of an object, for which we know only the graph states that characterize the buffers of the synthesized object. Many experiments indicate that carelessness with the Cartesian product may lead to the synthesis of the machine in the style of a "one-armed bandit" rather than to the synthesis of a properly functioning deterministic automaton with memory.

In the first example, the task is to synthesize the $G_X = G_1 \times G_2$ graph generated as a result of the multiplication of the graphs shown in Figs 5a, 5b, and 5c. In this example, we will unwittingly synthesize a falsely functioning graph state of an object with ambiguous mappings.

In the second example (Section 6), our carelessness will cause oscillatory behavior of the object with three buffers and a tendency toward unexpected relaxation on three objects A, B and C simulating or connected to object X with unstable functioning.

Returning to Example 1, the Cartesian product of the graphs G_1 and G_2 will be saved in the form of a signature model:

$$G_1 = < V_1, \Gamma V_1 >, G_2 = <V_2, \Gamma V_2 >, G_X = G_1 \times G_2$$

where:

$V_1 = \{a, b, c\}$, $V_2 = \{p, q\}$are the sets of the vertices of graphs G_1 and G_2,

$\Gamma_1 = \{\Gamma_a, \Gamma_b, \Gamma_c\}$, $\Gamma_2 = \{\Gamma_p, \Gamma_q\}$ are the signatures of the following graphs of the form:

$\Gamma_a = \{a, b\}$, $\Gamma_b = \{b, c\}$, $\Gamma_c = \{a, c\}$, $\Gamma_p = \{p, q\}$ and $\Gamma_q = \{q\}$.

The G_1, G_2 and G_x graphs are shown in Fig. 5a, 5b and Fig. 5c, respectively.

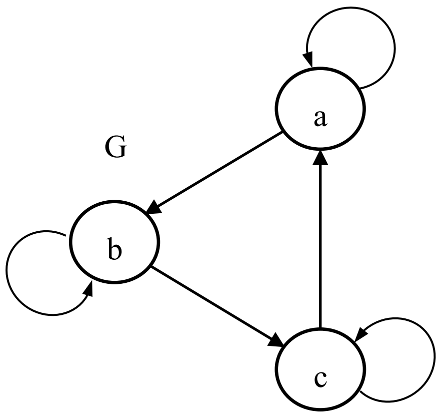

Figure 5a. State graph G_1

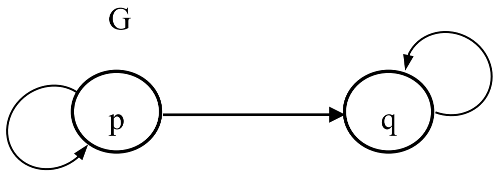

Figure 5b. State graph G_2

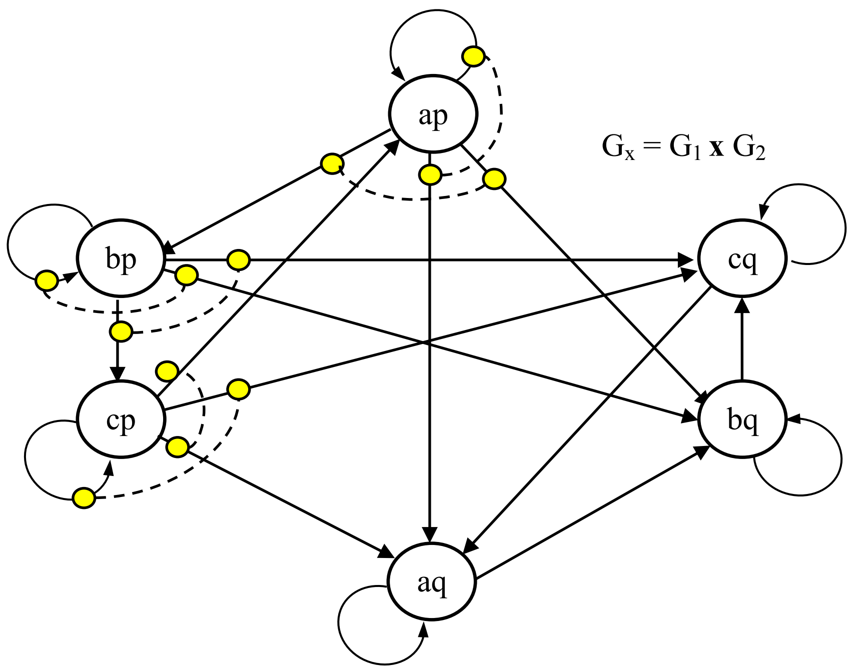

Figure 5c. State graph G_x (*Source:* Authors own research)

The carrier of the analyzed graph G_X is a set of six vertices obtained as the product of:

$V_x = V_1 \mathbf{x} V_2$

with identifiers {ap, bp, cp, aq, bq, cq}.

The signature of the vertices of the edge of the graph G_X is a set of six vertices of the graph:

$\{\Gamma_{ap}, \Gamma_{bp}, \Gamma_{cp}, \Gamma_{aq}, \Gamma_{bq}, \Gamma_{cq}\}$

forming edge bundles and loops.

Γ_{ap}	=	$\Gamma_a \times \Gamma_p$	=	{a, b} x {p, q}	=	{(a,p), (a,q), (b,p), (b,q)}
Γ_{aq}	=	$\Gamma_a \times \Gamma_q$	=	{a, b} x {q}	=	{(a,q), (b,q)}
Γ_{bp}	=	$\Gamma_b \times \Gamma_p$	=	{b, c} x {p, q}	=	{(b,p), (b,q), (c,p), (c,q)}
Γ_{bq}	=	$\Gamma_b \times \Gamma_q$	=	{b, c} x {q}	=	{(b,q), (c,q) }
Γ_{cp}	=	$\Gamma_c \times \Gamma_p$	=	{a, c} x {p, q}	=	{(a,p), (a,q), (c,p), (c,q)}
Γ_{cq}	=	$\Gamma_c \times \Gamma_q$	=	{a, c} x {q}	=	{(a,q), (c,q)}

The signatures of the above-mentioned vertices specify all the edges of the resulting graph G_X shown in Fig. 5c.

The graph G_X (Figs 5a, 5b and 5c) created as the Cartesian product of graphs G_1 and G_2 introduces an unexpected effect of uncertainty in the potential changes on the G_X graph. The indeterminacy effect is indicated by a dashed line of arcs connecting the pairs of alternative states and appears in the case of three states ap, bp and cp contained in the G_X column in Table 5. In Fig. 5c, we have three pairs showing nondeterministic behavior, marked in yellow, and this is presented in more detail in Table 5.

Table 5. Nondeterministic reactions of the G_x graph

Current G_x potential	New potential at entering the G_1 graph	Alternative G_x potentials
ap	a	ap
		aq
ap	b	bp
		bq
bp	b	bp
		bq
bp	c	cp
		cq
cp	a	ap
		aq
cp	c	cp
		cq

6 Tables of dynamics of two-buffer objects with an extensive structure of options

The series of event observation tables presented below is obtained from the ΓV signature of the graph shown in Figure 5c. The method for obtaining a stochastic state graph is analogous to the procedure described in Section 2. Black dots on the edges of the graphs indicate the right probability value assigned to the edge. The graphs G_1 and G_2, and the resulting graph G_X – taking into account the stable probability values – are presented in Figs 6a, 6b, and Fig. 6c.

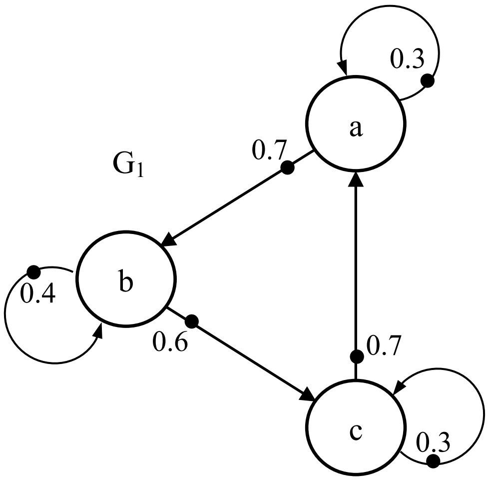

Figure 6a. State graph G_1
(*Source:* Authors own research)

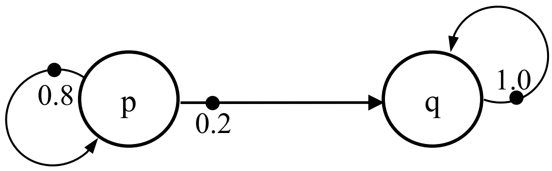

Figure 6b. State graph G_2
(*Source:* Authors own research)

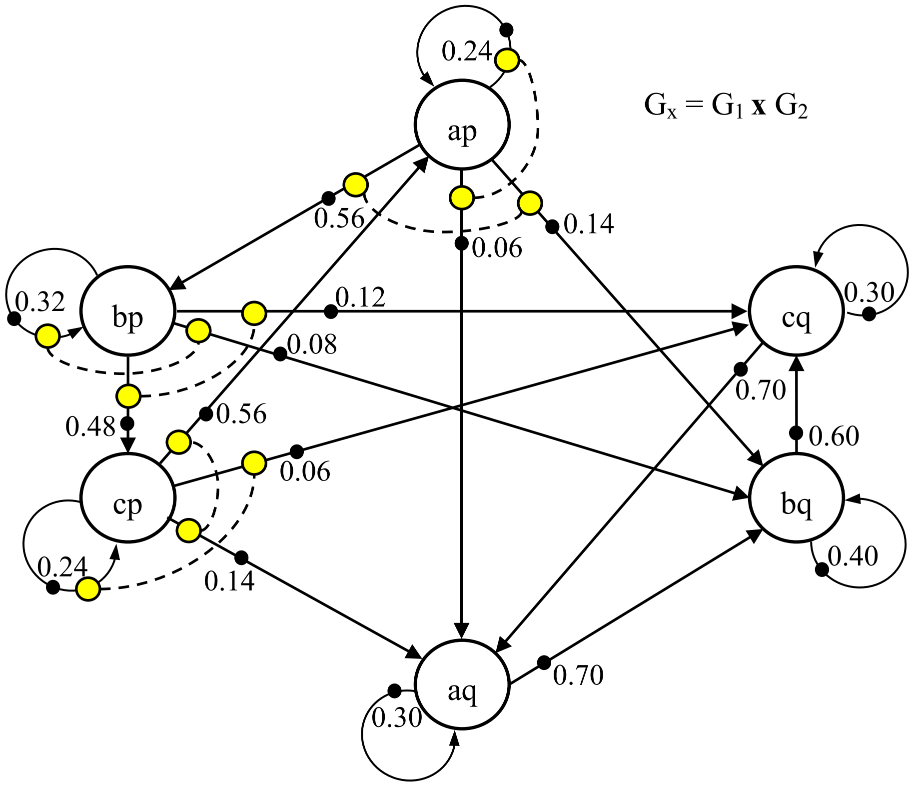

Figure 6c. State graph $G_X = G_1$ **x** G_2 (*Source:* Authors own research)

In the first example (Fig. 6a) we have synthesized an erroneously functioning graph state of the object with ambiguous mappings (marked in yellow). In the second example (Fig. 7a), our carelessness causes oscillatory behavior of the object with three buffers and a tendency toward the unexpected relaxation of the three objects A, B and C assigned to the object X with a similar functionality and unstable functioning.

The procedure leading to a stochastic graph G_X with the loss of unambiguity is analogous to the procedure for the dynamics tables of the two-buffer object, presented in Section 2. The results of the calculations are recorded in Tables 6 to 11.

In the procedure, establishing the set of vertices V_X obtained from the ΓV_X signature is the beginning:

$$\Gamma V_X = \Gamma V_1 \mathbf{x} \Gamma V_2 = \{a, b, c\} \mathbf{x} \{p, q\} = \{ap, aq, bp, bq, cp, cq\}$$

For each of signatures: Γ_{ap}, Γ_{bp}, and Γ_{cq}, the initiating event, the collections of secondary events and their statistical characteristics are set out in Tables 6 to 11.

$$\Gamma_{ap} = \Gamma_a \mathbf{x} \Gamma_p = \{a, b\} \mathbf{x} \{p, q\} = \{ap, aq, bp, bq\}$$
$$\Gamma_{aq} = \Gamma_a \mathbf{x} \Gamma_q = \{a, b\} \mathbf{x} \{q\} = \{aq, bq,\}$$
$$\Gamma_{bp} = \Gamma_b \mathbf{x} \Gamma_p = \{b, c\} \mathbf{x} \{p, q\} = \{bp, bq, cp, cq\}$$
$$\Gamma_{bq} = \Gamma_b \mathbf{x} \Gamma_q = \{b, c\} \mathbf{x} \{q\} = \{bq, cq\}$$
$$\Gamma_{cp} = \Gamma_c \mathbf{x} \Gamma_p = \{c, a\} \mathbf{x} \{p, q\} = \{cp, cq, ap, aq\}$$
$$\Gamma_{cq} = \Gamma_c \mathbf{x} \Gamma_q = \{c, a\} \mathbf{x} \{q\} = \{cq, aq\}$$

Table 6. Observation of event ap

Initializing event	Observation of secondary events	Probability P on the scale [0..1]
ap	ap→ap = 0.3 **x** 0.8	0.24
	ap→aq = 0.3 **x** 0.2	0.06
	ap→bp = 0.7 **x** 0.8	0.56
	ap→bq = 0.7 **x** 0.2	0.14
		Σ=1.00

Table 7. Observation of event aq

Initializing event	Observation of secondary events	Probability P on the scale [0..1]
aq	aq→aq = 0.3 **x** 1.0	0.30
	aq→bq = 0.7 **x** 1.0	0.70
		Σ=1.00

Table 8. Observation of event bp

Initializing event	Observation of secondary events	Probability P on the scale [0..1]
bp	bp→bp = 0.4 **x** 0.8	0.32
	bp→bq = 0.4 **x** 0.2	0.08
	bp→cp = 0.6 **x** 0.8	0.48
	bp→cq = 0.6 **x** 0.2	0.12
		Σ=1.00

Table 9. Observation of event bq

Initializing event	Observation of secondary events	Probability P on the scale [0..1]
bq	bq→bq = 0.4 **x** 1.0	0.40
	bq→cq = 0.6 **x** 1.0	0.60
		Σ=1.00

Table 10. Observation of event cp

Initializing event	Observation of secondary events	Probability P on the scale [0..1]
cp	cp→cp = 0.3 **x** 0.8	0.24
	cp→cq = 0.3 **x** 0.2	0.06
	cp→ap = 0.7 **x** 0.8	0.56
	cp→aq = 0.7 **x** 0.2	0.14
		Σ=1.00

Table 11. Observation of event cq

Initializing event	Observation of secondary events	Probability P on the scale [0..1]
cq	cq→cq = 0.3 **x** 1.0	0.30
	cq→aq = 0.7 **x** 1.0	0.70
		Σ=1.00

7 Cartesian product of graphs with lost semantics: Example 2

The task is to synthesize the graph G_X that is created as the Cartesian product of the graphs presented in Fig. 7a and saved in the form of the signature:

$$G_1 = < V_1 , \Gamma_1 >, G_2 = <V_2 , \Gamma_2 >, G_3 = <V_3 , \Gamma_3 >$$

where:

V_1 = {a, b}, V_2 = {c, d}, V_3 = {e, f} are the sets of vertices of graphs G_1, G_2 and G_3,

Γ_1, Γ_2 and Γ_3 are the signatures of the following graphs of the form:

$\Gamma_1 = \{\Gamma_a, \Gamma_b\}$, $\Gamma_2 = \{\Gamma_c, \Gamma_d\}$, $\Gamma_3 = \{\Gamma_e, \Gamma_f\}$,

Γ_a = (b), Γ_b = (a), Γ_c = (c,d),

Γ_d = (c), Γ_e = (f), Γ_f = (e).

The starting form of the graph is shown in Fig. 7a, and the resulting form in Fig. 7b.

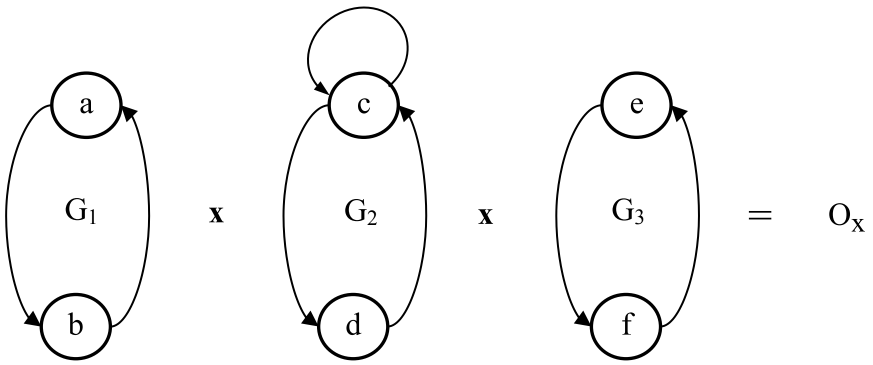

Figure 7a. The graph before attempting to synthesize the target form of the Cartesian product O_x
(*Source:* Authors own research)

The carrier of the graph G_X is the set of vertices:

$$V_x = V_1 \textbf{ x } V_2 \textbf{ x } V_3 = \{a, b\} \textbf{ x } \{c, d\} \textbf{ x } \{e, f\}$$

(a,d,e), (a,c,e), (b,d,e), (b,c,e), (a,d,f), (a,c,f), (b,d,f), (b,c,f).

Below the O_x's graph signature (Fig. 7b) is determined by the relationship "∨" alternative (ambiguous) links the edge of the graph in four highlighted gray background vertices of the graph: ace, bce, acf and bcf.

$\Gamma_{ade} = (b,c,f)$

$\Gamma_{ace} = (b,d,f) \vee (b,c,f)$

$\Gamma_{bde} = (a,c,f)$

$\Gamma_{bce} = (a,d,f) \vee (a,c,f)$

$\Gamma_{adf} = (b,c,e)$

$\Gamma_{acf} = (b,d,e) \vee (b,c,e)$

$\Gamma_{bdf} = (a,c,e)$

$\Gamma_{bcf} = (a,d,e) \vee (a,c,e)$

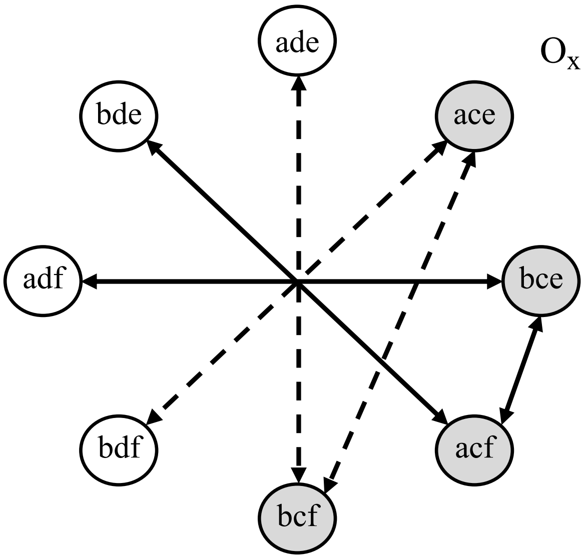

Figure 7b. A graph illustrating the Cartesian product O_x (*Source:* Authors own research)

In the O_X graph in Fig. 7b, it is not difficult to identify two intersecting graphical figures referred to as "wolf pits", which have the troublesome feature of the impossibility of leaving the graphical figure; we were inadvertently "caught up" in these in the modeling process:

♣ wolf pit No. 1: bde & acf & bce & adf,

and

♣ wolf pit No. 2: ade & bcf & ace & bdf.

A similar difficulty, caused by the lack of semantic analysis of the adopted assumptions, was encountered in the graph presented in Fig. 5b.

8 Summary and continuation using technology

The dominant concepts considered in this material are the mathematical signatures and the Cartesian products of graphs. The purpose of the signature of a graph is to specify, for each vertex of the graph:

- a set of edges of the graph with a common vertex and the creation of a set of vertices from the endpoints of each edge having a common vertex,
- it is possible that the signatures of different vertices of the graph will have common edge corners.

The Cartesian product of graphs is created in two phases:

- in the first phase, the Cartesian product of all possible vertex pairs, one from each of the sets, is found; in this way, the vertices of the new graph are created,
- in the second phase, for each new graph and its vertices, the signature is determined, that is, the final vertices and the edges leading to them.

The advantage of Cartesian products of graphs is that the vertices are merged simultaneously with the edges of the graph. This operation, even though it seems simple, can, however, quickly exhaust the available memory even with a small number of sets with a small number of elements in each of them. This hinders interpretation, which was also visible in our simple examples. We can see that there is an opportunity to use intelligent programming languages like Python or Java, as well as the work of those people of science who can overcome all these obstacles and achieve the goals.

9 Reference

[1] Domański, J., Kotarba, W., Krupa, T., 2014. The Prisms of Management. *Foundations of Management*. Vol. 6, No. 2, pp.43-50, DOI: 10.1515/fman-2015-0010.

[2] Banaszak, Z., Bocewicz, G., 2011. *Decision Support Driven Models and Algorithms of Artificial Intelligence*. Management Sciences Series, Vol. 1. Warsaw: Warsaw University of Technology, Faculty of Management.

[3] Gorbatov, V.A., 1979. *Semanticeskaja teorija projektirovanija avtomatov*. Moskva: Izd. Energija.

[4] Krupa, T., 2009. Events and Events Processes. *Foundations of Management*. Vol. 1, No. 2, pp.143-158, DOI: 10.2478/v10238-012-0016-9.

[5] Krupa, T., Ostrowska, T., 2007. Multilayer Decision Support Model for Value and Cost Analysis of IT Solutions – Hierarchical Approach. *Managing Worldwide Operations and Communications with Information Technology*. IGI Publishing, IRMA Int. Conf., Vancouver Canada, pp.86-90.

[6] Krupa, T., 2006. *Elementy organizacji, zasoby i zadania* (*Elements of Organization, Resources and Tasks*). Warszawa: WNT.

[7] Krupa, T., 2013. V.A. Gorbatov Theory of Characterization – Principles and Examples. *Foundations of Management*, Vol. 5, No. 3, pp.89-102, DOI: 10.2478/fman-2014-0022.

[8] Krupa T., 2018. The Principle of Characterization as a Systemic Paradigm of Safety: Experiments and Applications. *Foundations of Management*, Vol. 10, pp.303-318, DOI: 10.2478/fman-2018-0024.

[9] Krupa, T., Ostrowska, T., 2018. Security in Topological, Functional and Semiotic Terms. *Foundations of Management*, Vol. 10, pp.177-194, DOI: 10.2478/fman-2018-0024.

[10] Krupa, T., Kulińska, E., Ostrowska, T., Patalas-Maliszewska, J., Wiśniewski M., Zawiła-Niedźwiecki J., 2019. *Strategic Risk Management Against Hazards for Safety of Processes in Critical Infrastructures*. Management Sciences Series Vol. VIII, Copywright by Wydział Zarządzania, Politechnika Warszawska, ISBN 978-83-63370-20-6.

[11] Kulińska, E., 2016. Model of Axiological Dimension Risk Management. *Foundations of Management*, Vol. 8, No. 1, pp.211-226, http://dx.doi.org/10.1515/fman-2016-0017.

[12] Maj, K., 2007. Możliwość zastosowania sieci neuronowych w zarządzaniu sytuacją kryzysową, w przedsiębiorstwie elektroenergetycznym (The Possibility of Using Neural Networks in Crisis Management in a Power Company). *Zeszyty Naukowe - Nauki Ekonomiczne (Science Notebooks - Economics),* Kielce: Wydawnictwo Politechniki Świętokrzyskiej, pp.105-113.

[13] Maj, K., Krupa, T., 2010, The Management Method Preventing a Crisis Situation. *Foundation of Management*, Vol. 2, No. 2, pp. 37-50, https://doi.org/10.2478/v10238-012-0027-6.

[14] Ostrowska, T., 2013. The Resource Hazards Model for the Critical Infrastructure of the State Emergency Management Process. *Foundations of Management*, Vol.5, No. 3, pp.49-60. https://doi.org/10.2478/fman-2014-0019.

[15] Patalas-Maliszewska, J., Krupa, T., 2010. The Multicriteria Selection Methodology of the Decision Support System. *Foundations of Management*, Vol. 2, No. 2, pp.51-62. https://doi.org/10.2478/v10238-012-0028-5.

[16] Wiśniewski, M., 2016. Concept of Situational Management of Safety Critical Infrastructure of State. *Foundations of Management*, Vol. 08, pp.297-310, http://dx.doi.org/10.1515/fman-2016-0023.